Check for updates

View Article Online
View Journal

Journal of
Materials Chemistry A

Accepted Manuscript

This article can be cited before page numbers have been issued, to do this please use: C. Liu, C. Cao, J. Liu, X. Wang, Y. Zhu and W. Song, *J. Mater. Chem. A*, 2017, DOI: 10.1039/C7TA04187J.

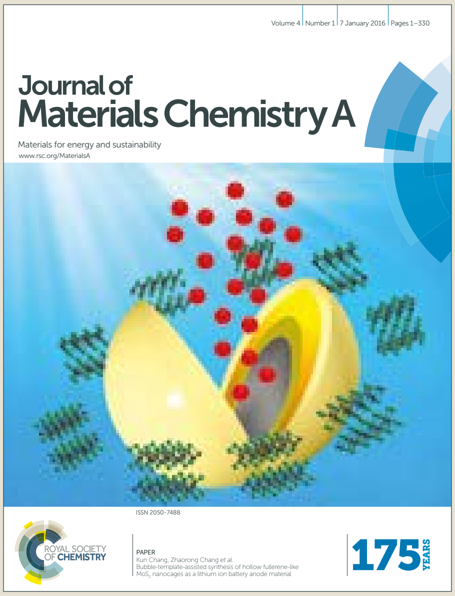

Volume 4 | Number 1 | 7 January 2016 | Pages 1–330

Journal of
Materials Chemistry A

Materials for energy and sustainability
www.rsc.org/MaterialsA

ISSN 2050-7488

ROYAL SOCIETY
OF CHEMISTRY

PAPER
Kun Chang, Zhaorong Chang *et al.*
Bubble-template-assisted synthesis of hollow fullerene-like MoS_2 nanocages as a lithium ion battery anode material

175 YEARS

This is an Accepted Manuscript, which has been through the Royal Society of Chemistry peer review process and has been accepted for publication.

Accepted Manuscripts are published online shortly after acceptance, before technical editing, formatting and proof reading. Using this free service, authors can make their results available to the community, in citable form, before we publish the edited article. We will replace this Accepted Manuscript with the edited and formatted Advance Article as soon as it is available.

You can find more information about Accepted Manuscripts in the author guidelines.

Please note that technical editing may introduce minor changes to the text and/or graphics, which may alter content. The journal's standard Terms & Conditions and the ethical guidelines, outlined in our author and reviewer resource centre, still apply. In no event shall the Royal Society of Chemistry be held responsible for any errors or omissions in this Accepted Manuscript or any consequences arising from the use of any information it contains.

ROYAL SOCIETY
OF CHEMISTRY

rsc.li/materials-a

View Article Online
DOI: 10.1039/C7TA04187J

Table of Contents

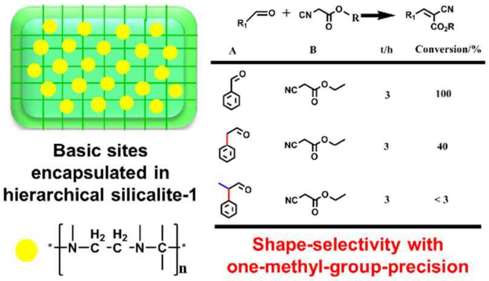

Shape-selectivity with one-methyl-group-precision can be realized in Knoevenagel condensation reactions on zeolite crystals encapsulating basic active sites.

View Article Online
DOI: 10.1039/C7TA04187J

Journal of Materials Chemistry A

ARTICLE

One Methyl Group Makes Major Difference: Shape-Selective Catalysis by Zeolite Nanoreactor in Liquid-Phase Condensation Reactions

Received 00th January 20xx,
Accepted 00th January 20xx

DOI: 10.1039/x0xx00000x

www.rsc.org/

Chang Liu, Changyan Cao*, Jian Liu, Xiaoshi Wang, Yanan Zhu and Weiguo Song*

The precise sizes of zeolites' micropores can induce sharp shape/size-selectivity with precisions less than 1 Å in gas-phase reactions, e.g. methanol to olefin reactions (MTO). However, it is still a major challenge and un-achieved task in the liquid-phase reactions. In this study, we demonstrate that shape-selectivity with one-methyl-group-precision can be realized in Knoevenagel condensation reactions on basic active sites encapsulated zeolite crystals. Furthermore, Pd nanoparticles can also be introduced to the interior of hollow zeolite crystals, resulting in a multifunctional and shape-selective catalyst in one-pot Knoevenagel condensation–hydrogenation cascade reaction.

Introduction

Zeolite is widely used in industry and research for its superior stability, various acid sites and well-defined pores[1-6]. Particularly, its well-defined micropores can differentiate molecules with precisions less than 1 Å [7], allowing it to be used in size-selective catalysis in the gas phase reactions. Their uniform pores with sizes in the range of 4-13 Å[8] are efficient in probing selectivity with substrates of comparable sizes[9].

Size-selective heterogeneous catalysts have been a long time goal in catalysis[10-15]. In 1965, Weitz et al selectively hydrogenated n-butanol at the presence of iso-butanol (difference in kinetic diameter less than 1Å) using acid zeolite catalyst[16]. Nowadays, a straight forward and effective strategy is to encapsulate metal nanoparticles in zeolite shell to form a multi-functional nanostructure. Xiao et al reported the direct synthesis of the Pd@S-1 complex in the presence of PVP stabilized Pd nanoparticles which showed impressive furan selectivity in the hydrogenation of biomass-derived furfural[17]. Li et al synthesized a series of Pd, Pt, Au nanoparticles inside the silicalite-1 to apply the size-selective catalysis in gas phase reactions[18,19]. Yu et al developed a synthetic protocol for encapsulating ultrasmall Pd clusters within nanosized silicalite-1 zeolite under direct hydrothermal conditions using soluble metal precursors[20].

Besides, other porous materials, like poly-dendrimers, MOF, COF, were studied in size-selective catalysis with their dense microporous structures[12,21-24]. However, most of these methods are restricted to metal nanoparticles, and the reaction was restricted to hydrogenation reaction[25]. Moreover, in the limited reports about size-selectivity in liquid-phase reactions, usually only two extreme scenarios were studied: very small substrate molecules that were fully converted and very large molecules that were unable to be converted[10,14,18]. No subtle selectivity change among slightly different molecules, such as one methylene or methyl group difference, was reported. Thus, it's particularly interesting to improve the multifunctional catalyst and expand their application in more reaction systems for size selective catalysis.

Knoevenagel condensation is of great significance in organic chemistry, producing key products essential for anionic polymerization and therapeutic drugs[26]. It is the condensation of aldehydes and malonic esters with active methylene group to form a new C-C bond on basic sites. Weak bases like primary, secondary, tertiary amine and ammonium salts under homogeneous conditions have been traditional catalysts for this reaction[27-29]. However, the recovery of conventional base catalysts is difficult and their utilization is associated with environmental pollution. Besides, homogeneous catalysts usually don't possess shape selectivity[30]. Thus, microporous zeolites with shape selectivity[31, 32] and encapsulated polymer with abundant ammine groups are ideal shape-selective catalyst for Knoevenagel condensation.

Inspired by the hollow silicalite-1 structure reported by Guo group[33-35], we fabricate a hierarchically porous (microporous shell and mesoporous core) nanoreactor with encapsulated

---

[a] *C. Liu, Dr. C. Cao, J. Liu, X. Wang, Y. Zhu, Prof. W. Song*
Beijing National Laboratory for Molecular Sciences
Laboratory of Molecular Nanostructures and Nanotechnology
CAS Research/Education Center for Excellence in Molecular Sciences
Institute of Chemistry, Chinese Academy of Sciences, Beijing 100190 (China)
E-mail: cycao@iccas.ac.cn, wsong@iccas.ac.cn
[b] *C. Liu, Dr. C. Cao, J. Liu, X. Wang, Y. Zhu, Prof. W. Song*
University of Chinese Academy of Sciences, Beijing 100049 (China)

† Footnotes relating to the title and/or authors should appear here.

Electronic Supplementary Information (ESI) available: [supporting figures]. See DOI: 10.1039/x0xx00000x

View Article Online
DOI: 10.1039/C7TA04187J

basic polymer through the "ship-in-a-bottle" method[36-38]. Combined with the alkaline polymer nanoparticles, the catalyst exhibits superior size-selectivity with one-methyl-group-precision toward Knoevenagel condensation reactions. In each case, a pronounced and subtle size-selectivity effect consistent with the pore dimensions was observed. Three groups of reactions were observed with about 100% conversion, 50% conversion and 0% conversion, respectively. And these results were explained by reactant or product shape-selectivity. Moreover, Pd nanoparticles can be introduced into the resultant and can be used in the hydrogenation of unsaturated nitrile, showing excellent activity and shape selectivity in one-pot Knoevenagel condensation–hydrogenation multistep cascade reaction.

Experimental

Synthesis of S-1 zeolite

Parent silicalite-1 zeolite was synthesized from the clear solution method with some modifications using a starting composition of 1 SiO_2:0.27 TPAOH:46 H_2O. 15 g TPAOH aqueous solution (25 wt%), 48 mL H_2O and 15.4 mL tetraethoxysilane (TEOS) was mixed and stirred at room temperature for 3 h to ensure complete TEOS hydrolysis to form a clear solution. The gel was then crystallized in a 100-mL Teflon-lined steel autoclave at 90 °C for 24 h. The product was recovered and calcined to remove the template in static air at 823 K for 8 h and denoted as S-1.

Synthesis of Polymers encapsulated in silicalite-1 zeolite shell (denoted as PHS-1)

0.5 g silicalite-1 was added into 15 mL of dichloromethane, then the mixture was added with 0.773 mL 3-aminopropyltrimethoxysilane (APTMS), and the slurry was stirred for 16 h at room temperature. Then the solid was recovered by centrifugation, washed and dried in the vacuum. The resulting mixture was treated with 0.5 M TPAOH water solution in an autoclave at 160 ^{o}C for 24 h to obtain a mesoporous core of the silicalite-1. Excess TPA^+ and OH^- was washed away to ensure purity of the material. Then the material was put into the tube furnace at 823 K for 8 h to remove the template. The obtained powder was mixed with 3.46 g carbon tetrachloride (CTC) and 1.56 g ethylenediamine (EDA). They were heated at 90ºC for 9 hours. After cooled down, it was washed with distilled water and ethanol ten times to make sure all the polymers attached to the outside of the zeolite was removed. After drying in a vacuum oven, polymers encapsulated in silicalite-1 zeolite shell was obtained.

Synthesis of Hierarchical mesoporous silicalite-1 nanospheres with different sized-mesopores (denoted as HS-1 (APTMS Concentration))

0.5 g silicalite-1 was added into 15 mL of dichloromethane, then the mixture was added with 0.515 mL, 0.644 mL, 0.773 mL 3-aminopropyltrimethoxysilane (APTMS), for HS-1 (0.164 M), HS-1 (0.205 M), HS-1 (0.246 M), respectively, and the slurry was stirred for 16 h at room temperature. Then the solid was recovered by centrifugation, washed and dried in the vacuum. The resulting mixture was treated with 0.5 M TPAOH water solution in an autoclave at 160 ^{o}C for 24 h to obtain a mesoporous core of the silicalite-1. Excess TPA^+ and OH^- was washed away to ensure purity of the material. Then the material was put into the tube furnace at high temperature to remove the template and denoted as HS-1.

Synthesis of The Polymers

CTC and EDA were mixed and heated at 90ºC for 9 hours. After cooled down, they were put in the vacuum oven to remove the rest liquid.

Synthesis of Pd nanoparticles loaded on Polymers inside silicalite-1 zeolite shell (denoted as Pd/PHS-1)

0.5 g PHS-1 was mixed with 2.575 mL Na_2PdCl_4 aqueous solution (0.0564 M) and stirred for 24 hours at RT. Then 70 mL of 0.15 M sodiumformate solution was added and the mixture stirred for 5 h. The solid was recovered by centrifugation and washed with distilled water for three times. After dried in an oven, Pd nanoparticles loaded on Polymers inside silicalite-1 zeolite shell was obtained.

Condensation reaction test

The size-selective catalysis was carried out in a glass reactor. Typically, 50 mg catalysts, 0.5 mmol benzaldehyde, 1mmol ethyl cyanoacetate and 10 mL methanol were put into a glass reactor (total volume: 25 ml). The reactor was heated at 50 ºC. Each hour the reaction sample was taken and analysed by GC-2010 Plus.

Condensation-hydrogenation reaction test

The size-selective catalysis was carried out in a Teflon-lined stainless steel reactor. Typically, 50 mg catalysts, 0.5 mmol cyclohexanone, 1mmol malononitrile and 10 mL methanol were put into the reactor (total volume: 25 ml). The reactor was sealed and purged with high-purity H_2 for three times under stirring to replace the air. Then the reactor was sealed and H_2 pressure was adjusted to 1 MPa. The autoclave was heated to 50 ºC and lasted for 1.5 hour. The reaction mixtures were filtered to remove catalyst particles, then the liquid was analyzed by GC (Shimadzu GC-2010) equipped with an ionization detector (FID) and an Rtx-5capillary column (0.25 mm in diameter, 30 m in length). The product was qualitatively determined by GC-MS (Shimadzu GCMS-QP2010S) with a HP-5MS capillary column (0.25 mm in diameter, 30 m in length).

Characterization

Scanning electron microscopy (SEM) images were obtained on a JEOL-6701F scanning electron microscope at 10.0 kV. Transmission electron microscopy (TEM) was carried out on a JEOL 2100F electron microscope operated at 200 kV. The XRD measurements were carried out in Shimadzu XRD-7000 diffractometer equipped with Cu Kα radiation (wavelengths λ =

View Article Online
DOI: 10.1039/C7TA04187J

0.154 nm). The hydrogenation products were measured using Shimadzu GC-2010 Plus (Rtx-5). Nitrogen adsorption-desorption isotherms was obtained on Quantachrome Autosorb AS-1. Elemental analysis was obtained on Flash EA 1112. X-ray photoelectron spectroscopy was obtained on VG ESCA Lab 220i-XL equipped with Mg/Al ultra-high vacuum X-ray binode-system. Thermogravimetric (TG) analysis was conducted on a SHIMADZU DTG-60 thermogravimetric analyzer. Temperature-programmed desorption (TPD) experiments were carried out on a Micromeritics Auto Chem II 2920 type instrument. Fourier transform infrared spectrum was performed on a TENSOR-27 type infrared spectrometer.

Results and discussion

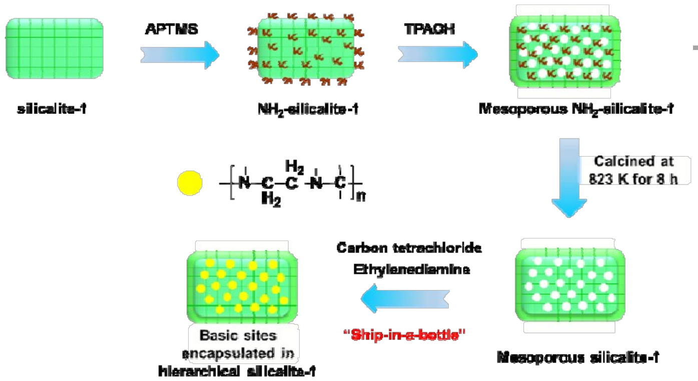

Scheme 1 Synthesis route of polymer nanoparticles encapsulated in silicalite-1 zeolite shell (PHS−1).

The synthesis route of polymer nanoparticles encapsulated in hierarchical silicalite-1 zeolite shell (denoted as PHS−1) mainly includes three steps (Scheme 1). First, silicalite-1 was modified with ammine group using 3-aminopropyltrimethoxysilane (APTMS). Then, with the protection of amino propyl group, interior mesopores were successfully generated by controlled silicon leaching under tetrapropylammonium hydroxide (TPAOH) treatment at 160 °C. Fig. S1 presented the TEM images of the hierarchical silicalite-1 zeolites (denoted as HS−1). When the concentration of APTMS used in the modifying procedure increased from 0.164 M to 0.246 M, the size of the mesopore decreased, along with the more even distribution of the mesopores (Fig. S1a-1c). A large hollow void is created in the interior of the silicalite-1 without APTMS treatment (Fig. S1d). These results demonstrated the role of amino propyl groups in the alkaline treatment procedure. With amino propyl groups evenly distributed in the zeolite, mesopores were formed inside the zeolite while the shell was intact and retained the microstructure of silicalite-1 after TPAOH etching. Finally, the composite was mixed with carbon tetrachloride (CTC) and ethylenediamine (EDA), and heated at 90 °C, encapsulating polymer nanoparticles into the interior mesopores. Since CTC and EDA molecules were small enough to diffuse in and out of the micropores, they formed polymer nanoparticles in the zeolite core. Meanwhile, the polymer nanoparticles were sufficiently large to stay inside the zeolite. The retained micropores of the zeolite wall is the origin of reactant, intermediates and product shape selectivity, while the encapsulated polymer is the base catalyst.

Transmission electron microscopic (TEM) images of PHS-1 are presented in Fig. 1. These images revealed that mesopores distributed inside the zeolites were uniform, indicating successful construction of mesoporous structure in the interior of S-1 zeolite single crystal. This alkaline-treated zeolite with abundant intra crystalline pores was an excellent platform for encapsulation of polymer nanoparticles. The embedded mesopores have a narrow size distribution in the range of 3.5–4.3 nm as estimated from the TEM images (Fig. 1a and Fig. S1f). SEM images of PHS-1 demonstrated that the zeolite shell was intact (Fig. S2). Elemental mapping images (Fig. 1c-1f) showed that the polymer nanoparticles (mainly from element N and Cl) were evenly dispersed within the hierarchical porous nanospheres.

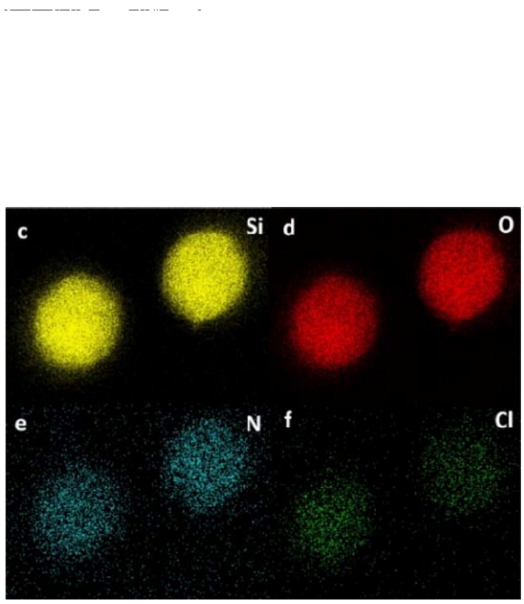

Fig. 1 (a) Bright field TEM image of PHS-1; (b) Dark field TEM image of PHS-1; (c) Si Kα1, (d) O Kα1, (e) N Kα1 and (f) Cl Kα1 EDS elemental mappings of PHS−1.

The crystallinity and phase composition of the materials were characterized using wide-angle X-ray diffraction (WAXRD). As shown in Fig. 2a, the XRD pattern of PHS-1 matched well with those of S-1 and HS-1, which illustrated PHS-1 still maintained its original crystal structure after alkali treatment and polymer encapsulation. The porosity of the core−shell catalyst was further confirmed by Nitrogen adsorption−desorption isotherms, as shown in Fig. 2b. The sample displayed a type IV isotherm, confirming the mesoporous structure of PHS-1. The Brunauer−Emmett−Teller (BET) surface area and pore volume were calculated to be 267.4 $m^2{\cdot}g^{-1}$ and 0.30 $cm^3{\cdot}g^{-1}$, respectively, which was apparently lower than that of S-1 and HS-1. The Nitrogen adsorption-desorption isotherms of S-1 and HS-1 was shown in Fig. S3. The decrease of BET surface area and pore volume was attributed to the presence of dense cross-linked polymers that occupied the inner mesopores. From the pore size analysis

View Article Online
DOI: 10.1039/C7TA04187J

(inset of Fig. 3b), the PHS-1 had a rather narrow pore size distribution centred at 3.7 nm.

The FTIR spectrum of PHS-1 contained the characteristic peaks of S-1 (Fig. 2c). The band at 1085 cm^{-1} and 804 cm^{-1} can be assigned to the Si–O–Si asymmetric and symmetric stretching vibrations, respectively. Besides, the appearance of absorption bands at 3400 cm^{-1} corroborated with Si-OH stretching and bending vibrations on the surface of the zeolite. The internal and external asymmetric stretching modes of vibrations were also observed at 1105 cm^{-1} and 1230 cm^{-1}, respectively. For the polymers, the band at around 3400 cm^{-1}, 2920 cm^{-1}, 1110 cm^{-1} was attributed to amine groups (–NH–)[39], alkyl groups (–CH$_2$–)[40] and C–N groups[41], respectively. Above results indicated that the polymer nanoparticles were encapsulated in the interior of zeolites.

Fig. 2 (a) XRD patterns of S-1, HS-1 and PHS-1; (b) Nitrogen adsorption-desorption isotherms of PHS-1; (c) FTIR spectrums of PHS-1 and the pure polymer; (d) Carbon dioxide TPD spectra of PHS-1.

Temperature-programmed desorption with CO$_2$ (CO$_2$-TPD) as probe molecule was conducted to test the basicity of the catalyst. CO$_2$ desorption bands were observed between 230 °C and 300 °C for PHS-1 (Fig. 2d). Typically, the desorption temperature is an indication of the basic site strength, and higher desorption temperature suggests stronger basicity. Therefore, PHS-1 exhibited very high basicity when comparing with other amines functionalized catalysts, which was in agreement with the total amounts of adsorbed CO$_2$ (Fig. S4a). Thermogravimetric analysis (Fig. S4b) showed that there was about 14% weight loss from 100 °C to 700 °C for PHS-1, indicating its stability in liquid-phase reactions.

In order to investigate the size-selectivity of PHS-1, Knoevenagel condensation reaction was chosen due to the basicity of the encapsulated polymer. Meanwhile, the pure polymer was also used for comparison. Eight substrates were tested (Table 1) and they were classified into three groups according to their different conversions (Fig. S5a). In the first group, complete conversions and nearly 100 % yields were obtained in a few hours when Benzaldehyde (0.43×0.60 nm) or p-tolualdehyde (0.43×0.68 nm) reacted with ethyl cyanoacetate (0.47×0.65 nm) (Table 1, entries 1-3 and Fig. S5b).

Table 1 Knoevenagel condensation reaction sequences towards different substrates using PHS-1 as catalyst

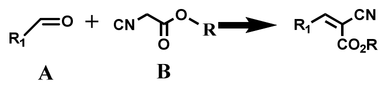

Entry	A	B	t/h	Conversion/%
1	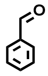	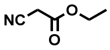	3	100
2	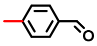	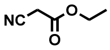	3 3.5	93 100
3	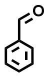	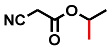	3 6	73 98
4	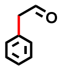	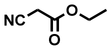	3 24	40 54
5	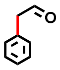	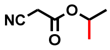	3 24	20 40
6	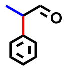	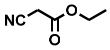	3 24 60	< 3 ~ 6 < 8
7	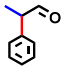	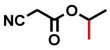	3 24 60	< 3 ~ 8 < 10
8	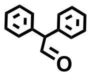	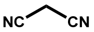	3 24 60	< 3 ~ 9 < 10

Reaction conditions: Aldehyde (A) (0.5 mmol), Nitrile (B) (1 mmol), MeOH (10 mL), catalyst (50 mg). 50 ºC. Conversion and yield were determined by GC analysis using para-xylene as internal standard. The conversion is all based on Aldehyde (A).

In the second group, the conversion of phenylacetaldehyde (0.43×0.72 nm) or isopropyl 2-cyanoacetate (0.47×0.61 nm) only reached up to 54 % conversion no matter how long the reaction lasted (Table 1, entries 4-5 and Fig. S5c). In the third group, for 2-fenyl-1-propanal (0.44×0.73 nm), ethyl cyanoacetate (0.47×0.65 nm) and isopropyl 2-cyanoacetate (0.47×0.61 nm), which were all smaller than micropores, less than 3% conversion was observed after 3 hours (Table 1, entries 6-7 and Fig. S5d). In addition and as expected, diphenylacetaldehyde (0.96×0.73 nm) reacted very little because its size is larger than the zeolite micropores (Table 1, entry 8 and Fig. S5d). The little conversions in entries 6-8 were probably attributed to the residue basic sites on the outer surface of S-1. For comparison, all above reactions reached 100 % conversion within 1 h on pure polymer catalyst, proving that the basicity of the polymer was high enough for the condensation reactions listed above. The diffusion barrier imposed by the zeolite micropore was accounted for the observed reactivity difference.

The size-selectivity performance of PHS-1 catalyst could be directly attributed to the molecular sieving characteristics of silicalite-1. Because the size of silicalite-1 micropores (0.53×0.56 nm) is larger than that of benzaldehyde (0.43×0.60 nm), p-tolualdehyde (0.43×0.68 nm), ethyl cyanoacetate (0.47×0.65 nm) and isopropyl 2-cyanoacetate (0.47×0.61 nm), the mass transfer of them in liquid-phase solution was facile, and 100 % conversion was reached within hours. However, subtle reaction rate difference was observed. In the first group, the reaction rates reduced distinctly when the size of the reactant molecules enlarged slightly by adding a methyl group to benzene ring or to the ester (Fig. S5b). It illustrated that the size-selectivity of the catalyst was quite sensitive as to recognize one carbon difference on the molecule chain.

In the second group (Fig. S5c), the reaction was slower and the conversion reached a plateau at about 54% conversion. A possible reason for the 54% conversion was that reactant, intermediate or product molecules were adsorbed on the surface of micropores, leading to the block of the pores. Thus, no reactants could approach the polymer, no intermediates could form and no products could transport from the zeolites. It was very interesting that phenylacetaldehyde only had one more methylene group than phenylacetaldehyde, which was in the first group, and there was significant conversion difference (Table 1, entry 1 & 4).

In the third group (Fig. S5d), though 2-fenyl-1-propanal could move in and out of the micropores with ease, there was no product detected. The main reason was that the product molecules were too large to diffuse out of the micropores, showing an example of product shape selectivity. In addition, the minimum size of diphenylacetaldehyde (0.96×0.73 nm) was significantly larger than that of silicalite-1 micropores, it was unable to diffuse through the shell and enter the cavity to reach active sites of polymer nanoparticles. Thus, no conversion was observed.

These results also confirmed that nearly all polymer nanoparticles were located inside the zeolite, and all composite catalyst had integral structure (no broken zeolite). The micropores not only differentiate the size of the reactant molecules, but also the product molecules. The results demonstrated that the shape-selective catalysis for different size of reactant molecules could be adjusted effectively by the micropore in the shell of PHS-1.

Moreover, Pd nanoparticles can be introduced into the PHS-1 (denoted as Pd/PHS-1). The synthesis route is shown in Scheme S1. Transmission electron microscopic (TEM) images of Pd/PHS-1 are presented in Fig. S6, which showed that the ultra-small Pd nanoparticles were evenly distributed inside the zeolite, owing to the binding of the Pd nanoparticles to the amine groups at the surface of the polymer. XRD pattern of Pd/PHS-1 matched well with those of S-1 and PHS-1 (Fig. S7b). The obtained Pd/PHS-1 can be used in one-pot Knoevenagel condensation–hydrogenation multistep cascade reaction. Cyclohexanone and Malononitrile were converted to Cyclohexanemalononitrile in 1.5 h, affording excellent activity. However, for 2-phenyl-1-propanal and ethyl cyanoacetate, diphenylacetaldehyde and malononitrile, there was no hydrogenation product detected. Such result was expected as no Knoevenagel condensation reaction occurred between these two molecules.

Conclusions

We produced a multifunctional catalyst by combining the hierarchically porous (microporous shell and mesoporous core) zeolite with basic polymer nanoparticles. The catalyst exhibited superior size-selectivity with one-methyl-group-precision towards Knoevenagel condensation reactions. Because of the micropores on the zeolite shell, it not only differentiates the size of the reactant molecules, but also the product molecules, leading to a three distinct groups of reactions. Furthermore, Pd nanoparticles can be introduced into the resultant, generating it as a multifunctional and shape-selective catalyst for one-pot Knoevenagel condensation–hydrogenation cascade reaction. This structure will be a useful platform for fabricating more stable, multifunctional, and recyclable and green catalysts applied in shape/size-selective reactions and one-pot cascade reactions.

Acknowledgements

We thank the financial supports from the National Natural Science Foundation of China (NSFC 21333009, 21273244, 21573245), Chinese Academy of Sciences-Peking University Pioneer Cooperation Team and the Youth Innovation Promotion Association of CAS (2017049).

References

1 C. Baerlocher, L. B. McCusker, Database of Zeolite Structure: http://www.izastructure.org/databases/.
2 A. Corma, V. Fornes, S. B. Pergher, T. L. M. Maesen and J. G. Buglass, *Nature*, 1998, **396**, 353. 6 Citations should appear here in the format A. Name, B. Name and C. Name, *Journal Title*, 2000, **35**, 3523.
3 V. Van Speybroeck, K. Hemelsoet, L. Joos, M. Waroquier, R. G. Bell and C. R. Catlow, *Chem. Soc. Rev.*, 2015, **44**, 7044.
4 T. Ennaert, J. Van Aelst, J. Dijkmans, R. De Clercq, W. Schutyser, M. Dusselier, D. Verboekend and B. F. Sels, *Chem. Soc. Rev.*, 2016, **45**, 584.
5 J. Shi, Y. Wang, W. Yang, Y. Tang and Z. Xie, *Chem. Soc. Rev.*, 2015, **44**, 8877.
6 A. Corma, *Chem. Rev.*, 1995, **95**, 559.
7 M. E. Davis, *Industr. & Engineer. Chem. Res.*, 1991, **30**, 1675.
8 M. E. Davis and R. F. Lobo, *Chem. Mater.*, 1992, **4**, 756.
9 M. E. Davis, *Acc. Chem. Res.*, 1993, **26**, 111.
10 Z. A. Qiao, P. Zhang, S. H. Chai, M. Chi, G. M. Veith, N. C. Gallego, M. Kidder and S. Dai, *J. Am. Chem. Soc.*, 2014, **136**, 11260.
11 Z. Shang, R. L. Patel, B. W. Evanko and X. Liang, *Chem. Commun.*, 2013, **49**, 10067.
12 L. Lin, T. Zhang, X. Zhang, H. Liu, K. L. Yeung and J. Qiu, *Industr. & Engineer. Chem. Res.*, 2014, **53**, 10906.
13 J. Gu, Z. Zhang, P. Hu, L. Ding, N. Xue, L. Peng, X. Guo, M. Lin and W. Ding, *ACS Catalysis*, 2015, **5**, 6893.
14 C. Liu, J. Liu, S. Yang, C. Cao and W. Song, *ChemCatChem*, 2016, **8**, 1279.
15 S.-K. Oh, Y. Niu and R. M. Crooks, *Langmuir*, 2005, **21**, 10209.

View Article Online
DOI: 10.1039/C7TA04187J

16 P. B. Weisz, V. J. Frilette, R. W. Maatman and E. B. Mower, *J. Catal.*, 1962, **1**, 307.
17 C. Wang, L. Wang, J. Zhang, H. Wang, J. P. Lewis and F. S. Xiao, *J. Am. Chem. Soc.*, 2016, **138**, 7880.
18 S. Li, T. Boucheron, A. Tuel, D. Farrusseng and F. Meunier, *Chem. Com mun.,* 2014, **50**, 1824.
19 S. Li, L. Burel, C. Aquino, A. Tuel, F. Morfin, J. L. Rousset and D. Farrusseng, *Chem. Commun.,* 2013, **49**, 8507.
20 N. Wang, Q. Sun, R. Bai, X. Li, G. Guo and J. Yu, *J. Am. Chem. Soc.,* 2016, **138**, 7484.
21 Q. Fang, S. Gu, J. Zheng, Z. Zhuang, S. Qiu and Y. Yan, *Angew. Chem. Int. Ed.*, 2014, **53**, 2878.
22 W. Zhang, G. Lu, C. Cui, Y. Liu, S. Li, W. Yan, C. Xing, Y. R. Chi, Y. Yang and F. Huo, *Adv. Mater.*, 2014, **26**, 4056.
23 K. Albrecht, Y. Kasai, Y. Kuramoto and K. Yamamoto, *Chem. Commun.,* 2013, **49**, 865.
24 X. Wang, M. Li, C. Cao, C. Liu, J. Liu, Y. Zhu, S. Zhang and W. Song, *ChemCatChem*, 2016, **8**, 3224.
25 D. Farrusseng and A. Tuel, *New J. Chem.*, 2016, **40**, 3933.
26 G. Marciniak, A. Delgado, G. Leclerc, J. Velly, N. Decker and J. Schwartz, *J. Med. Chem.*, 1989, **32**, 1402.
27 E. Knoevenagel, *Euro J. Inorg. Chem.*, 1894, **27**, 2345.
28 J. March, *Advanced Organic Chemistry*, 4th edn., Wiley, Chichester, 1992.
29 L. F. Tietze, U. Beifuss, in: B.M. Trost (Ed.), *Comprehensive Organic Synthesis*, Pergamon, Oxford, 1991.
30 J. M. Lee, Y. Na, H. Han and S. Chang, *Chem. Soc. Rev.,* 2004, **33**, 302.
31 P. Collier, S. Golunski, C. Malde, J. Breen and R. Burch, *J. Am. Chem. Soc.,* 2003, **125**, 12414.
32 H. Yang, Y. Chong, X. Li, H. Ge, W. Fan and J. Wang, *J. Mater. Chem.*, 2012, **22**, 9069.
33 C. Dai, A. Zhang, J. Li, K. Hou, M. Liu, C. Song and X. Guo, *Chem. Commun.,* 2014, **50**, 4846.
34 C. Dai, A. Zhang, L. Li, K. Hou, F. Ding, J. Li, D. Mu, C. Song, M. Liu and X. Guo, *Chem. Mater.*, 2013, **25**, 4197.
35 C. Dai, A. Zhang, M. Liu, L. Gu, X. Guo and C. Song, *ACS Nano*, 2016, **10**, 7401.
36 W. Song, J. F. Haw, *Angew. Chem. Int. Ed.,* 2003, **42**, 892.
37 A. Fukuoka, N.Higashimoto, Y. Sakamoto, M. Sasaki, N. Sugimoto, S. Inagaki, Y. Fukushima, M. Ichikawa, *Catal. Today*, **2001**, *66*, 23.
38 Herron, Norman, *Journal of Coordination Chemistry*, 1988, **19**, 25.
39 A. Pielesz and A. Włochowicz, *Spectrochimica Acta Part A: Molecular and Biomolecular Spectroscopy*, 2001, **57**, 2637.
40 R. M. F. Lima, P. R. G. Brandão and A. E. C. Peres, *Minerals Engineering*, 2005, **18**, 267.
41 Y. Sun, C. Cao, P. Huang, S. Yang and W. Song, *RSC Adv.*, 2015, **5**, 86082.